(1)

RL-TR-94-69
Final Technical Report
June 1994

ASYMMETRIC COUPLED QUANTUM WELLS FOR HIGH SPEED OPTICAL MODULATORS AT COMMUNICATION WAVELENGTHS

University of Arizona

B.P. McGinnis, Sergey Ten,
and N. Peyghambarian (University of Arizona)

Mark F. Krol, Michael J. Hayduk, Steven T. Johns,
and Douglas A. Norton (Rome Laboratory)

APPROVED FOR PUBLIC RELEASE; DISTRIBUTION UNLIMITED.

Rome Laboratory
Air Force Materiel Command
Griffiss Air Force Base, New York

This report has been reviewed by the Rome Laboratory Public Affairs Office (PA) and is releasable to the National Technical Information Service (NTIS). At NTIS it will be releasable to the general public, including foreign nations.

RL-TR-94-69 has been reviewed and is approved for publication.

APPROVED:

MARK F. KROL
Project Engineer

FOR THE COMMANDER:

LUKE L. LUCAS, Colonel, USAF
Deputy Director
Surveillance & Photonics Directorate

REPORT DOCUMENTATION PAGE

Form Approved
OMB No. 0704-0188

1. AGENCY USE ONLY (Leave Blank)	2. REPORT DATE	3. REPORT TYPE AND DATES COVERED
	June 1994	Final Jan 93 - Jan 94

4. TITLE AND SUBTITLE
ASYMMETRIC COUPLED QUANTUM WELLS FOR HIGH SPEED OPTICAL MODULATORS AT COMMUNICATION WAVELENGTHS

5. FUNDING NUMBERS
C - F30602-93-C-0005
PE - 62702F
PR - 4600
TA - P1
WU - PJ

6. AUTHOR(S)
B.P. McGinnis, Sergey Ten, and N. Peyghambarian (U. of Arizona); Mark F. Krol, Michael J. Hayduk, Steven T. Johns, and Douglas A. Norton (Rome Laboratory)

7. PERFORMING ORGANIZATION NAME(S) AND ADDRESS(ES)
University of Arizona
Optical Sciences Center
Tucson AZ 85721

8. PERFORMING ORGANIZATION REPORT NUMBER
N/A

9. SPONSORING/MONITORING AGENCY NAME(S) AND ADDRESS(ES)
Rome Laboratory (OCPA)
25 Electronic Pky
Griffiss AFB NY 13441-4515

10. SPONSORING/MONITORING AGENCY REPORT NUMBER
RL-TR-94-69

11. SUPPLEMENTARY NOTES
Rome Laboratory Project Engineer: Mark F. Krol/OCPA/(315) 330-4456

12a. DISTRIBUTION/AVAILABILITY STATEMENT
Approved for public release; distribution unlimited.

12b. DISTRIBUTION CODE

13. ABSTRACT (Maximum 200 words)
A novel design for electro-optic modulators operating at wavelengths compatible with fiber-based optical interconnects and networks is presented. This design uses InGaAs/InAlAs asymmetric coupled quantum wells (ACQWs) to enhance the electro-optic effect within the material and results in a low power modulator capable of high-speed operation. A device was fabricated which shows real charge transfer between the ACQWs. This device shows that without modulation doping and real charge transfer the quantum confined stark effect in InGaAs/InAlAs is insufficient to provide strong modulation at low drive voltages. Standard pump-probe techniques were also used to study the dynamics of charge transfer between the wells. Picosecond recovery times were exhibited by these devices and were found to be independent of the barrier width.

14. SUBJECT TERMS
electro-optic modulators, InGaAs/InAlAs asymmetric coupled quantum wells (ACQWs)

15. NUMBER OF PAGES
24

16. PRICE CODE

17. SECURITY CLASSIFICATION OF REPORT	18. SECURITY CLASSIFICATION OF THIS PAGE	19. SECURITY CLASSIFICATION OF ABSTRACT	20. LIMITATION OF ABSTRACT
UNCLASSIFIED	UNCLASSIFIED	UNCLASSIFIED	SAR

ACKNOWLEDGMENTS

This report is the result of collaborative research accomplished by the Rome Laboratory Photonics Center under in-house research project 4600P213 and the University of Arizona under Rome Laboratory contract number F30602-93-0005.

The project was conceived and initiated by Rome Laboratory personnel. Mark Krol, Michael Hayduk, Steven Johns and Doug Norton were the laboratory personnel involved in the effort. The personnel from the University of Arizona were Dr. Peyghambarian, Dr. McGinnis and Sergy Ten.

We wish to thank Hyatt Gibbs and Galina Khitrova at the University of Arizona for fabrication of several of the samples. Also special thanks to Rich Leavitt of Army Research Laboratory for sample fabrication.

Table of Contents

Asymmetric coupled quantum wells for high speed optical modulators at communication wavelengths

B. P. McGinnis, Sergey Ten, and N. Peyghambarian

Optical Sciences Center, University of Arizona, Tucson, AZ 85721

Mark F. Krol, Michael J. Hayduk, Steven T. Johns, and Douglas A. Norton

Rome Laboratory Photonics Center, Griffiss Air Force Base, NY 13441

1.0 Introduction

Ultra-fast fiber-based optical interconnects and networks will require the use of fast and efficient electro-optic modulators and switches in the near future. The application of these optical technologies will depend on compatibility with existing electronic technology and compactness of required components. Currently, there are many novel fiber-based optical interconnect and network architecture's that have demonstrated the advantages of using optics instead of electronics to transmit data. These architecture's have demonstrated high optical data throughput where the data has remained in optical form throughout the switching fabric, i.e. no optical-to-electronic and vise versa conversion is required. However, the control of the switch has been left entirely to the domain of electronics. This fact has forced systems engineers to use existing electro-optic technology to implement systems test beds. Electro-optic technology is required at all electrical to optical interfaces, i.e. modulators and switches. The most attractive existing technology which satisfies systems engineers needs is lithium niobate technology. Although this technology has been well developed, its application to optical systems which must interface directly to electronics (TTL, ECL circuits) is questionable due to the large power requirements of these components when operated at gigahertz data rates. A device which must interface with an electronic circuit and requires one or two watts of RF power at a couple of gigahertz cannot be used in any real-world application.

In this report, we demonstrate an electro-optic technology which may offer an attractive alternative to using power hungry electro-optic technologies, such as lithium niobate, in optical interconnect and network applications. The technology relies on the large tool box of optical nonlinearities available with the interaction of light with semiconductor materials.[1] Indeed the physics of light-semiconductor interactions has been well documented. However, little semiconductor optics research has been performed on materials and devices, with the exception of lasers and detectors, which are compatible with existing optical fiber spectral characteristics. Here, we demonstrate the use of InGaAs/InAlAs asymmetric coupled quantum wells as potential materials and devices for applications which require efficient electro-optic components. The report is organized in four sections: 2.1) Modulator Concept and Design, 2.2) Steady-State Electron Transfer, 2.3) Dynamic Response, and 2.4) Conclusions.

2.0 Summary of Results

2.1 Modulator Concept and Design

Although semiconductors can offer large electro-optic nonlinearities near the semiconductor bandedge, materials relevant to fiber-based optical communications offer rather small electro-optic nonlinearities. The nonlinearity mainly responsible for electro-absorption and electro-refraction in semiconductor multiple quantum well (MQW) materials is the quantum confined Stark effect (QCSE). In GaAs/AlGaAs MQWs the QCSE is largely due to the large electron and hole effective masses and freedom to choose arbitrarily large well widths.[2] In the GaAlInAs system required for optical communications applications, the QCSE is quite small. The primary reason for the lack of a large QCSE is the reduced electron and heavy hole masses in these materials and the restriction of available well widths.[3] For fiber-based optical communication systems, the materials and devices must be compatible with the 1.3 and 1.55 μm transmission windows of optical fibers. For GaInAs/AlInAs on InP MQW systems this requires well sizes to be 40Å and 70Å, respectively. It should be stressed that there is no flexibility in these widths without changing the composition of the ternary well material to a quaternary material.

Shown in Fig. 1 is electro-absorption data for a MQW sample with 40Å and 70Å well sizes. As expected a two step absorption profile is observed. The heavy and light

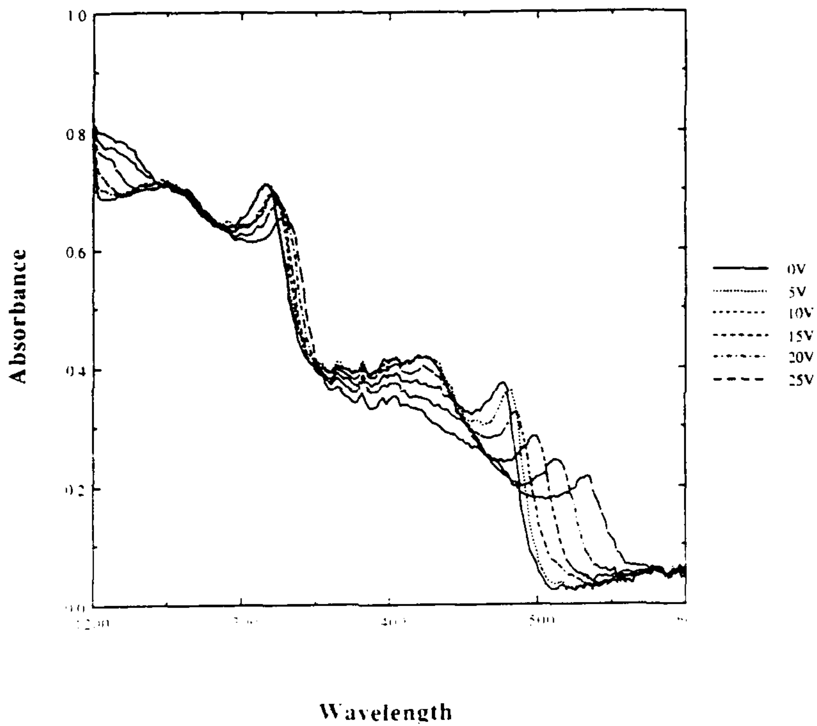

Figure 1. Room temperature absorption spectra of ACQW in PIN diode for different applied bias voltages. The two step-like transitions are due to wells of both narrow (40Å) and wide (70Å) widths. Notice the large voltage needed to get significant shift due to the QCSE.

excitonic transitions are clearly resolved at each step. The short wavelength set of excitonic peaks are associated with the lowest allowed transitions in the 40Å (narrow) well and the long wavelength set of excitonic peaks are associated with the lowest allowed transitions in the 70Å (wide) well. As can be seen in the figure, with increasing applied voltage, the excitonic features show a corresponding red-shift and broadening of their respective spectral characteristics. A remarkable feature is the drastic difference in the magnitude of these changes between the narrow and wide wells. The difference is due to the larger confinement of the narrow well; hence, the electron and hole wavefunction cannot be separated to the extent of those in the wide well. The shift of both the narrow and wide well excitonic features is quadratic. This effect is thus called the *Quadratic Stark Effect*. It has been shown that the shift of the hole and electron levels follows the law $\Delta E = m^*F^2L^4$, where m* is the electron or hole effective mass, F is the field strength, and L is the well width.[4] Another important result has just been shown, the quadratic Stark effect is dependent on the fourth power of the well width. If this data was compared with GaAs/AlGaAs MQW systems, the absorption change per applied field is much larger since wider wells can be used for applications which require GaAs-based materials. Finally, the intrinsic region width of the GaInAs/AlInAs MQW sample was approximately 1 μm. Hence, for large absorption changes to be obtained in these materials, fields strengths on the order of 2.5×10^5 V/cm must be applied to these materials. For a device application which requires gigahertz operating speeds, a voltage swing of 25 V into a 50 ohm load is unacceptable. Clearly, an alternative solution must be found.

An attractive solution is the use of asymmetric coupled quantum well materials where an excess carrier distribution is intentionally formed (either by optical excitation or modulation doping) in the wide well only (see Fig. 2). The presence of the excess charge density bleaches the absorption near the bandedge of the wide well. When a field is applied, the lowest level in the wide well conduction band can be placed above the lowest level in the narrow well conduction band. When this condition is reached, the excess charge (electrons in this case) localized in the wide well will tunnel from the wide well to narrow well. As a result, the absorption near bandedge of the wide well will recover.

To study the electro-optic effects induced by an excess charge density in an asymmetric coupled quantum well (ACQW) structure, two sets of samples were designed and fabricated. The first was a PIN structure grown by MBE on an n+ InP substrate. The epi-layers where grown in the following order from the substrate up: 0.35 μm Si-Doped

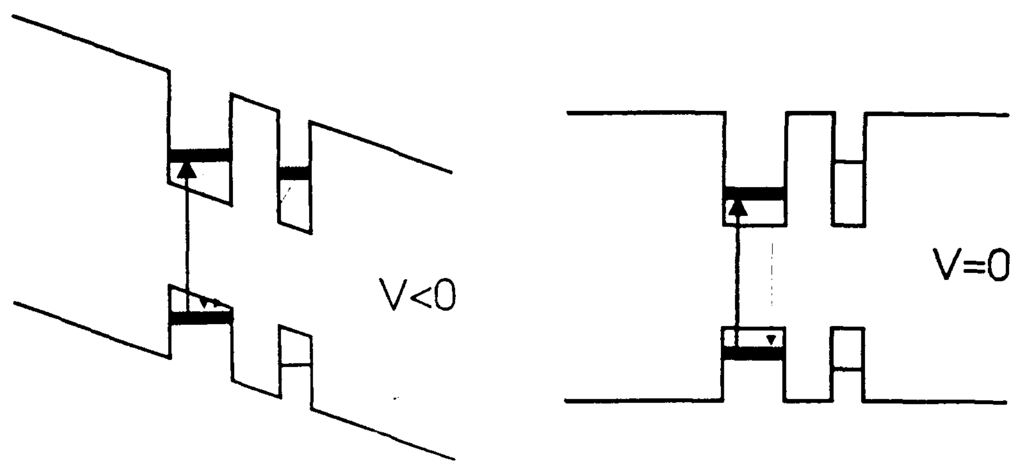

Figure 2. Schematic band structure both with and without applied bias of the doped ACQW modulator. Transfer of charge from the wide to narrow well with applied bias allows large changes in the optical transitions due to band filling effects while requiring lower drive voltages. Since charge transfer is only internal to the structure, modulation frequencies will be only limited by tunneling rates between adjacent wells.

$Al_{0.48}In_{0.52}As$, n = $2x10^{18}$ cm^{-3}; 0.15 μm $Al_{0.48}In_{0.52}As$; 30 periods of 10 nm $Al_{0.48}In_{0.52}As$/ 7 nm $Ga_{0.47}In_{0.53}As$/ 3.5 nm $Al_{0.48}In_{0.52}As$/ 4.0 nm $Ga_{0.47}In_{0.53}As$; 0.15 μm $Al_{0.48}In_{0.52}As$; 0.2 μm Be-Doped $Al_{0.48}In_{0.52}As$, p = $2x10^{18}$ cm^{-3}; 20 nm p+ $Ga_{0.47}In_{0.53}As$ contact layer.

The second set of ACQW samples without a PIN structure were grown by MBE on semi-insulating InP substrates. The epi-layers were grown in the following order from the substrate up: $Al_{0.48}In_{0.52}As$ buffer; 60 periods of 4 nm $Ga_{0.47}In_{0.53}As$/ L_b nm $Al_{0.48}In_{0.52}As$/ 6.0 nm $Ga_{0.47}In_{0.53}As$/ 15 nm $Al_{0.48}In_{0.52}As$; $Ga_{0.47}In_{0.53}As$ cap; where L_b = 2.5, 3.5, 4.5, and 10 nm respectively.

The first sample will be used to study the steady-state electron transfer between the wide and narrow wells, and the second set of samples was used to study the temporal dynamics of the electron transfer process. In particular, the transfer rate as a function of barrier width is extremely important for the design of an optimized modulator structure.

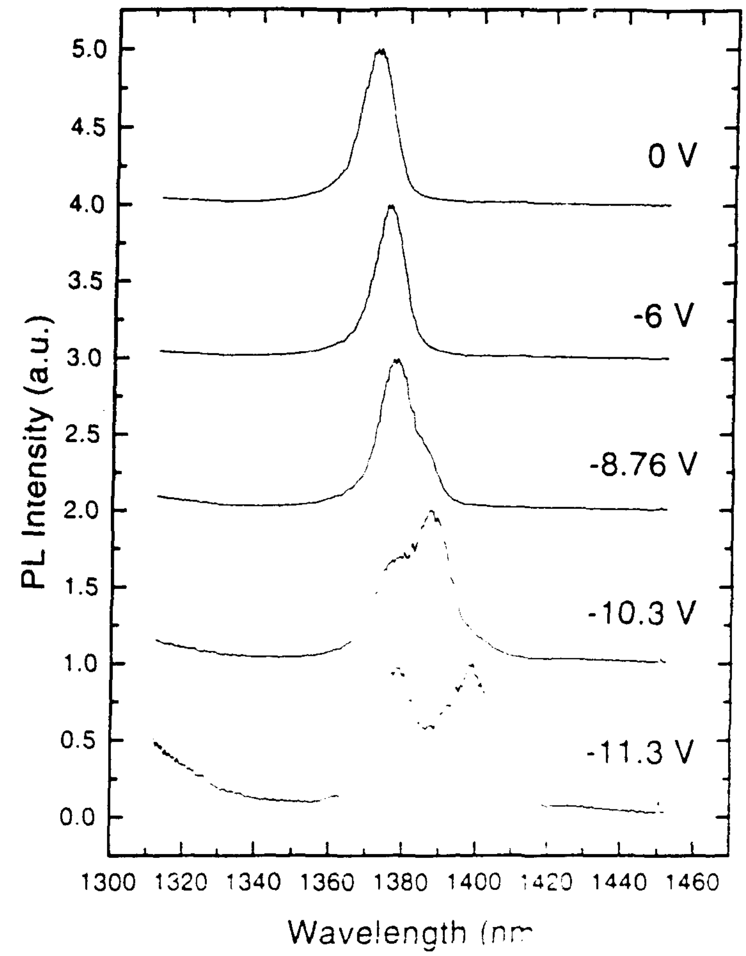

Figure 3. CW photoluminescence spectra at different applied biases from undoped ACQW in PIN diode optically pumped on the wide well absorption. The new emission peak appearing at biases greater than -8.76 V indicates strong transfer of electrons from the wide to narrow well with cross-transitions becoming available.

2.2 Steady-State Electron Transfer

To study the steady-state electron transfer process in ACQWs, continuous-wave photoluminescence (CW PL) was utilized. Although CW PL in a common technique, the experimental arrangement used here in unique in the fact that we used a CW Cr:forsterite laser as the pump source. The forsterite laser offers the capability to pump samples in the 1.2 to 1.3 μm region. For the present study, the ability to pump only the wide well is imperative since this is how a charge density localized in the wide well was generated. The experimental setup is a standard CW PL arrangement. The PIN sample described above was mounted in a closed-cycle helium cryostat. The sample was held at a constant temperature of 8.5 K throughout the steady-state measurements. As already discussed, the sample was pumped by tuning the forsterite laser to 1275 nm, i.e. a wavelength between the lowest allowed transition in the narrow well (1238 nm) and lowest allowed transition in the wide well (1370 nm); hence, electrons and holes were only generated in *the wide well.* The PL from the sample was then detected by a spectrometer/InGaAs linear diode array/OMA combination.

The measured PL as a function of applied bias voltage from the sample is shown in Fig. 3. At zero applied bias, only one PL peak is observed corresponding the wide well heavy-hole exciton transition. As the reverse bias is increased, the main PL peak shows a slight Stark Shift to longer wavelengths; however, when the applied reverse bias reaches a value of approximately -8.2 volts, a splitting of the single PL peak into two peaks is observed. At an applied voltage of -8.2 volts, the two lowest electron levels in the narrow and wide wells shift into resonance. The splitting of the PL peak at this voltage is a result of the anti-crossing of the two levels. The splitting indicates that the electrons, which were once totally localized in the wide well are now de-localized over both the wide and narrow well. Further evidence of the electron de-localization is seen when the reverse bias is increased. For applied biases of greater than -8.2 volts, the second peak becomes clearly separated from the initial PL peak. In fact, as the bias is increased, the second peak shows a continual shift to longer wavelengths.

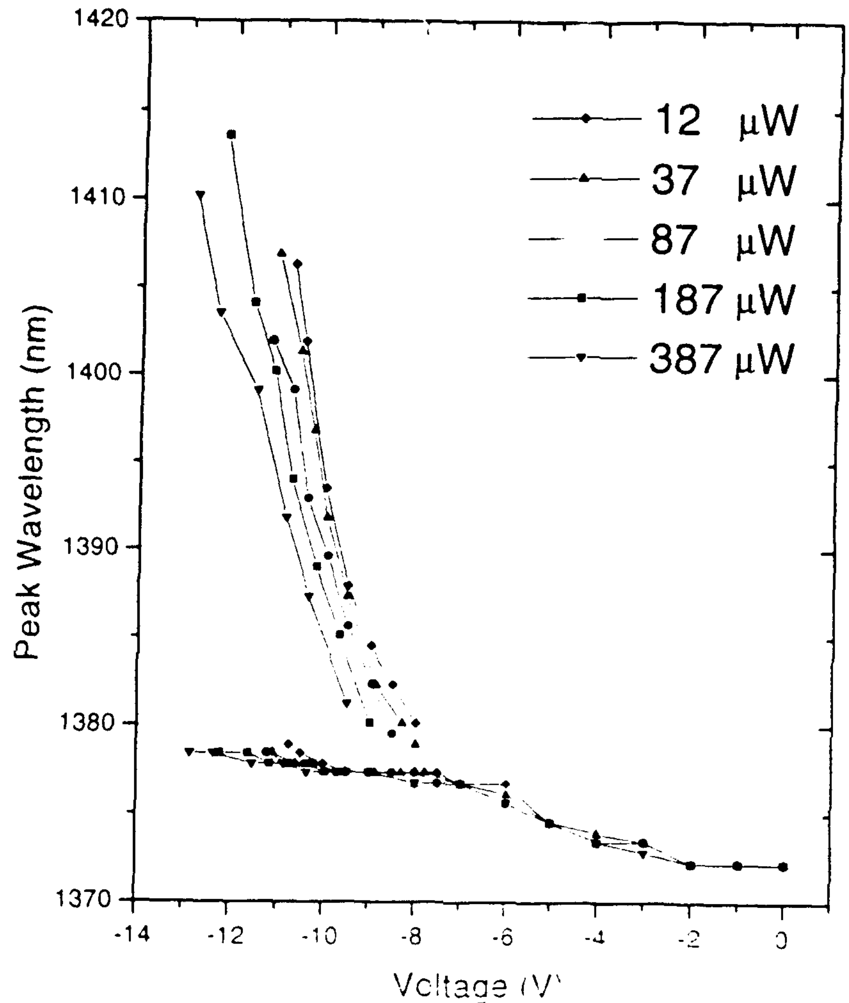

Figure 4. CW PL peak positions as a function of optical pump intensities showing the effects of space-charge buildup.

Figure 4 illustrates the shift of the long wavelength peak as a function of reverse bias for different pump powers. As the applied field approaches the resonance voltage, the single PL peak splits into two peaks. The long wavelength peak shows a dramatic shift to longer wavelengths. In fact the shift is approximately linear with increasing reverse bias. The second peak can be attributed to a spatially indirect transition between electrons localized in the narrow well and holes localized in the wide well. It should be noted that the matrix element for this transition is small due to the spatially localized wavefunctions of the electrons and holes; hence, the density of transferred electrons must be large in order for a large PL signal at this transition to be present. An interesting effect is also observed as the pump power is increased. For increased pump powers, the voltage at which the indirect transition splits off increases due to the build-up of a space-charge field which screens the applied field. The space-charge field is the result of the localization of electrons and holes in separate wells.[5,6]

Although these effects have been observed in GaAs/AlGaAs ACQW systems,[7] this is the first time electron transfer in GaInAs/AlInAs ACQWs has been demonstrated. Finally, we have demonstrated the ability to control the spatial location of an optically generated charge density. As a result, the excess charge can be used to control the absorption strength of the lowest energy transitions in either the wide or narrow wells. However, the transfer rate of excess carriers must also be investigated and is the topic of the next section.

2.3 Dynamic response

The fundamental time that limits the modulation response of the ACQW modulator structure is the transfer time of carriers between the quantum wells. While in a real device, parasitic resistance and capacitance will actually limit the modulation dynamics, it is important to know the fundamental transfer time within the quantum well material. To that end, we have designed and grown undoped ACQW's as described above to measure the transfer time of carriers between wells as a function of barrier width between the wells. Since the transfer time between wells is described by the quantum mechanical tunneling time through the barrier, we can model the behavior and compare the experimental recovery times with those of our model.

The experimental method for measuring the tunneling times between wells used an optically-degenerate pump and probe technique. A modelocked Nd:YLF laser at

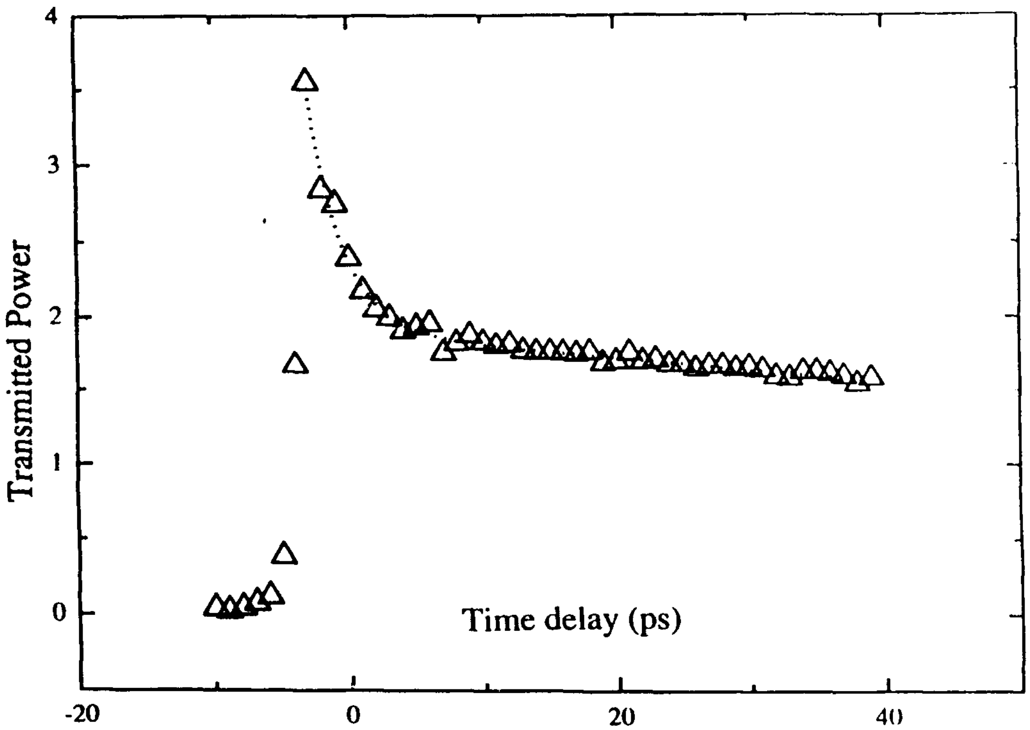

Figure 5. Typical optical pump and probe recovery dynamics of ACQW with a barrier width of 35Å.

1.315 μm was split into orthogonal-polarized pump and probe beams. With the samples held at room temperature, the photon energy of this laser pumps and probes transitions just above the lowest narrow well absorption resonance. As electrons and holes from the narrow well transfer to the wide well, the absorption of the narrow well recovers. By varying the time delay between the pump and probe pulses, this recovery is measured by monitoring the transmission of the probe pulse. The measurement is repeated for all four intrinsic ACQW samples to characterize the recovery as a function of barrier width.

The recovery times show a biexponential character, as exemplified in Fig. 5. This is consistent with different tunneling times for the electrons and holes. The widest barrier (L_b = 10 nm) shows no recovery of the narrow well resonance over a few hundred picosecond time. This is consistent with the thick barriers isolating the narrow and wide wells so that little tunneling occurs between the wells. The thinner barriers (L_b = 4.5, 3.5, and 2.5 nm) show a surprising result. The fast decays which we associate with the electrons show no dependence on barrier thickness. The decay times are approaching the resolution of our present experimental equipment of approximately one picosecond. While we cannot yet explain these fast electron decay times, picosecond recovery indicates fundamental modulation frequencies near a terahertz.

In studies of intersubband tunneling in materials such as GaAs/AlGaAs ACQWs, the tunneling process was dominated by polar longitudinal optical (LO) phonon emission and absorption.[8] Due to similarities in materials, for the initial theoretical analysis of the tunneling process in the GaInAs/AlInAs ACQWs studied here polar LO phonon emission and absorption was also considered as the dominant tunneling mechanism. The theory of intersubband scattering in MQWs has been well developed. For this work, we followed the formalism developed by *Price.*[9] The theory uses Fermi's Golden rule to calculate the transition rate between subbands and assumes the electrons confined in the ACQW structure are interacting with bulk GaInAs LO phonon modes. The results of these calculations along with the measured tunneling times are shown in Fig. 6. The calculated curve indicates that the tunneling time should have a logarithmic dependence on barrier width. However, the measured tunneling times show no barrier width dependence. In order to verify our calculations, we checked our model against published calculations for GaAs/AlGaAs ACQWs in which the tunneling process was dominated by polar LO phonon/electron interaction. We found good agreement between the calculations performed *Muto, et al* and our calculations.[8]

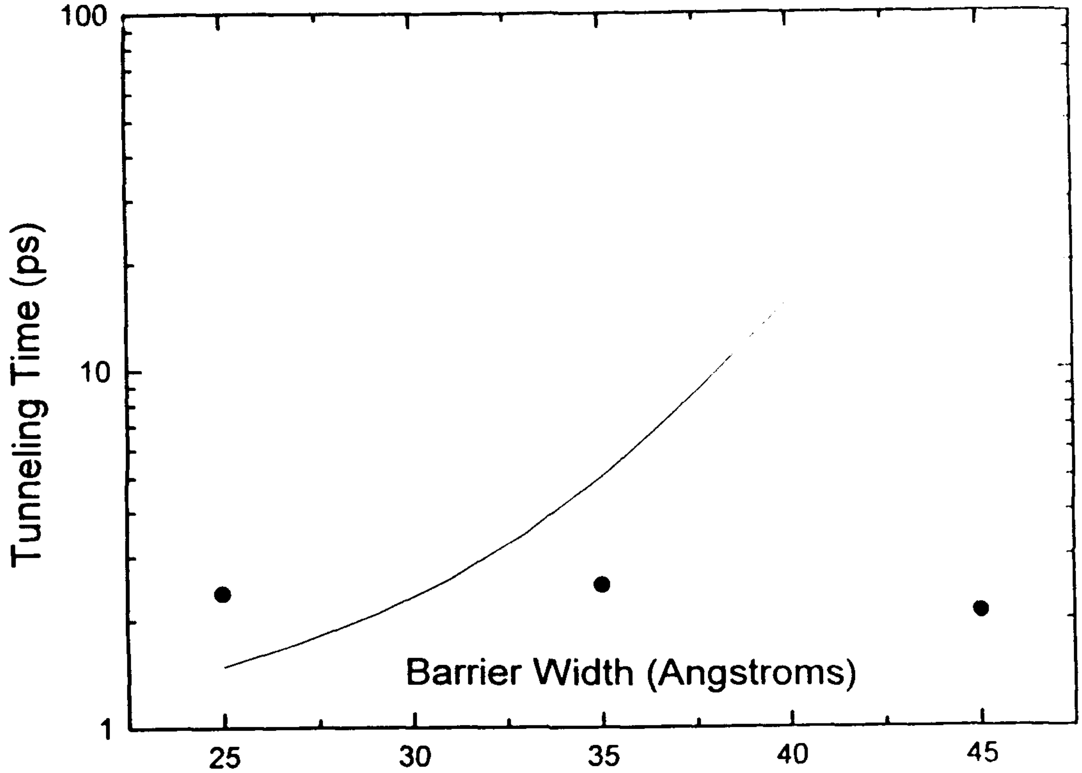

Figure 6. Fast component of tunneling times as a function of barrier width along with expected times from LO phonon tunneling.

The primary difference between the GaInAs/AlInAs and GaAs/AlGaAs materials is the ternary system is a disordered alloy while the binary system is a perfect crystal. To account for alloy scattering in our model, we calculated the alloy scattering times using the Fermi Rule formalism.[10] The tunneling times were found to be in the regime of hundreds of picoseconds; thus, the possibility of alloy scattering significantly contributing to the measured tunneling times was ruled out. One important point should be mentioned, both LO phonon and alloy scattering have a logarithmic dependence on the barrier width since both processes rely on the overlap integral of the electron probability density functions (not probability amplitude functions).

One process that has not been fully considered at this time is interface scattering. Interface scattering may not show any barrier width dependence since the scattering process is localized to the regions near GaInAs/AlInAs interfaces. The large discrepancy between the measured tunneling times and the calculated times (only including those processes mentioned) indicates the tunneling process in the GaInAs/AlInAs ACQW system may rely on a different fundamental process than that found in GaAs/AlGaAs ACQWs. Clearly, the more complicated crystal structure of the ternary materials may lead to processes such as interface scattering dominating the tunneling process while in binary materials these processes are absent. Hence, this study has uncovered some interesting effects which are the topic of a continuing study.

3.0 Conclusion

We have presented the designs for a new electro-optic modulator for use at communications wavelengths. This design incorporates real charge transfer kinetics within the material to enhance the electro-optic effect and reduce the required drive voltages. This will result in a modulator with reduced power requirements at high-speed operation. We have constructed a device which shows that real charge transfer between the wells does occur and results in CW PL spectra which agree well with the expected level shifts with applied voltage. This device also shows that without modulation doping and real charge transfer the QCSE in these materials is insufficient to provide strong modulation with low drive voltages.

With these real charge devices, the dynamics of the charge distribution between wells will fundamentally limit the modulation frequency. A series of undoped wells were designed and grown to study the dependence of charge transfer times on barrier width. Using a picosecond laser, we optically injected carriers into the wells and characterized the recovery dynamics of the ACQWs. We found picosecond recovery times which indicate very fast transfer dynamics of the electrons. The transfer rates were quite insensitive to the barrier width. These results indicate that very high modulation frequencies, nearing terahertz, are possible with this design and that tolerances for the barrier width are very relaxed.

The relative independence of tunneling times on barrier width was an unexpected result and was not predicted by LO phonon assisted tunneling. While this model works quite well for the GaAs/AlGaAs material system, additional mechanisms must contribute in this material system used for communication wavelengths. These results indicate that further investigation of the ternary materials need to be performed. Many of the previous results obtained in the binary materials may not apply to the ternary materials we are using for the communication wavelengths. We intend to continue investigations along these lines, such as comparing equivalent binary and ternary compound ACQW structures in addition to further development and optimization of the modulator design.

4.0 References

1. N. Peyghambarian, S. W. Koch, and A. Mysyrowicz, *Introduction to Semiconductor Optics*, (Prentice Hall, Englewood Cliffs, NJ, 1993).
2. J. S. Weiner, D. A. B. Miller, D. S. Chemla, T. C. Damen, C. A. Burrus, T. H. Wood, A. C. Gossard, and W. Wiegmann, Appl. Phys. Lett. **47**, 1148 (1985).
3. R. P. Leavitt, J. W. Little, and S. C. Horst, Phys. Rev. B **40**, 4183 (1989).
4. G. Bastard, *Wave Mechanics Applied to Semiconductor Heterostructures*, (Halsted Press, NY, 1988).
5. N. Vodjdani, B. Vinter, V. Berger, E. Böckenhoff, and E. Costard, Appl. Phys. Lett. **59**, 555 (1991).
6. R. Sauer, K. Thonke, and W. T. Tsang, Phys. Rev. Lett. **61**, 609 (1988).
7. J. W. Little and R. P. Leavitt, Phys. Rev. B **39**, 1365 (1989).
8. S. Muto, T. Inata, A. Tackeuchi, Y. Sugiyamam, and T. Fujii, Appl. Phys. Lett. **58**, 2393 (1991).
9. P. J. Price, Annals of Physics **133**, 217 (1981).
10. S. Muckhopadhyay and B. R. Nag, Appl. Phys. Lett. **60**, 2897 (1992).

MISSION

OF

ROME LABORATORY

Mission. The mission of Rome Laboratory is to advance the science and technologies of command, control, communications and intelligence and to transition them into systems to meet customer needs. To achieve this, Rome Lab:

a. Conducts vigorous research, development and test programs in all applicable technologies;

b. Transitions technology to current and future systems to improve operational capability, readiness, and supportability;

c. Provides a full range of technical support to Air Force Materiel Command product centers and other Air Force organizations;

d. Promotes transfer of technology to the private sector;

e. Maintains leading edge technological expertise in the areas of surveillance, communications, command and control, intelligence, reliability science, electro-magnetic technology, photonics, signal processing, and computational science.

The thrust areas of technical competence include: Surveillance, Communications, Command and Control, Intelligence, Signal Processing, Computer Science and Technology, Electromagnetic Technology, Photonics and Reliability Sciences.